PII: S0032-3861(97)00143-2

Polymer Vol. 38 No. 23, pp. 5775–5783, 1997

0032-3861/97/$17.00 + 0.00

Vapour–liquid equilibria for some binary and ternary polymer solutions

John O. Tanbonliong and John M. Prausnitz*
Department of Chemical Engineering, University of California, Berkeley, and Chemical Sciences Division, Lawrence Berkeley National Laboratory, Berkeley, CA 94720, USA
(Received 4 December 1996)

Vapour–liquid equilibrium (VLE) data for seven binary polymer + solvent systems and for one ternary polymer + mixed solvent system have been obtained using the gravimetric–sorption method at 50°C. The binary polymer + solvent mixtures studied include polystyrene (PS), poly(methyl methacrylate) (PMMA) and the random copolymer poly(styrene-*co*-50% methyl methacrylate) in acetone, methyl acetate and chloroform. Solvent absorption by the copolymer was inbetween those by PS and PMMA for chloroform, but it was less than those by either homopolymer for acetone and methyl acetate. A modification to the classic gravimetric–sorption technique was established for acquiring sorption data for polymer + mixed solvent systems. VLE data were obtained for polystyrene + chloroform + carbon tetrachloride. A perturbed hard-sphere chain (PHSC) equation of state was used to correlate binary and ternary VLE data. © 1997 Elsevier Science Ltd.

(Keywords: vapour–liquid equilibria; gravimetric sorption; molecular thermodynamics)

INTRODUCTION

Vapour–liquid equilibrium (VLE) data for polymer + solvent systems are useful for a variety of applications including recovery of organic vapours using polymeric membranes[1,2], surface acoustic-wave vapour sensors[3,4], polymer devolatilization[5], vapour-phase photografting[6] and pervaporation[7]. For efficient and effective process design and control, the VLE behaviour of polymer + solvent systems must be accurately characterized through experimental data or molecular thermodynamic correlations.

Although VLE data for copolymer + solvent systems[8,9] are rare compared to those for homopolymer + solvent systems[10], copolymers are increasingly used in the manufacture of numerous materials. The solution properties of copolymers are of special interest in polymer blends and may have potential for new separation process applications. Because interactions between the monomer units of a copolymer influence the solution properties of copolymers in a polymer blend[11,12], this work contributes new VLE data for copolymer + solvent mixtures towards a better understanding of molecular interactions in these systems. In this work, binary polymer + solvent VLE data have been obtained at 50°C for poly(styrene-*co*-50% methyl methacrylate) (P(S-*co*-MMA)) random copolymer and its parent homopolymers polystyrene (PS) and poly(methyl methacrylate) (PMMA) with several solvents. Recent VLE studies have suggested that some solvents can be more soluble in a copolymer than in the parent homopolymers of the copolymer if the solvent molecules relieve repulsive forces among incompatible monomer units in the copolymer[13]. However, as shown later, the opposite effect has been observed here for P(S-*co*-MMA) in some solvents.

Very few VLE data are available for ternary mixtures containing one polymer and two volatile solvents. Experimental studies for such systems are difficult. We describe here a method for acquiring ternary VLE data using a modification of the classic gravimetric–sorption technique. A VLE apparatus has been constructed to acquire both binary and ternary data. Experimental VLE results were obtained for PS + chloroform + carbon tetrachloride at 50°C. All binary and ternary data were correlated using a perturbed hard-sphere chain (PHSC) equation of state.

EXPERIMENTAL

Materials

Table 1 gives the weight-average molecular weight (M_w), polydispersity factor, glass transition temperature, and commercial sources of all polymers used. The glass transition temperature of the copolymer was calculated using the Fox–Flory equation

$$\frac{1}{T_g} = \frac{F_1}{T_{g1}} + \frac{F_2}{T_{g2}} \quad (1)$$

where T_g is the glass-transition temperature of the copolymer, T_{g1} and T_{g2} are the glass-transition temperatures of the parent homopolymers, and F_1 and F_2 are the mass fractions of the parent monomers. Acetone and chloroform were obtained from Fisher Scientific (Pittsburgh, PA, USA) while methyl acetate and carbon tetrachloride were from Aldrich Chemical (Milwaukee, WI, USA). These solvents had purities greater than 99%; they were used without further purification.

* To whom correspondence should be addressed

Table 1 Polymer characteristics and solvent vapour pressures at 50°C

Polymer	M_w^a	M_w/M_n^b	T_g (°C)[c]	Supplier
PS	50 000	1.05	100	Polysciences, Inc., Warrington, PA, USA
PMMA	125 000	1.05	110	Polymer Source, Inc., Dorval, Quebec, Canada
P(S-*co*-MMA)	100 000	<1.1	105	Polysciences, Inc., Warrington, PA, USA

Solvent	Vapour pressure at 50°C (kPa)
Acetone	81.67
Methyl acetate	78.69
Chloroform	70.17
Carbon tetrachloride	41.59

[a] Weight-average molecular weight
[b] Polydispersity factor; M_n is the number-average molecular weight
[c] Glass transition temperature

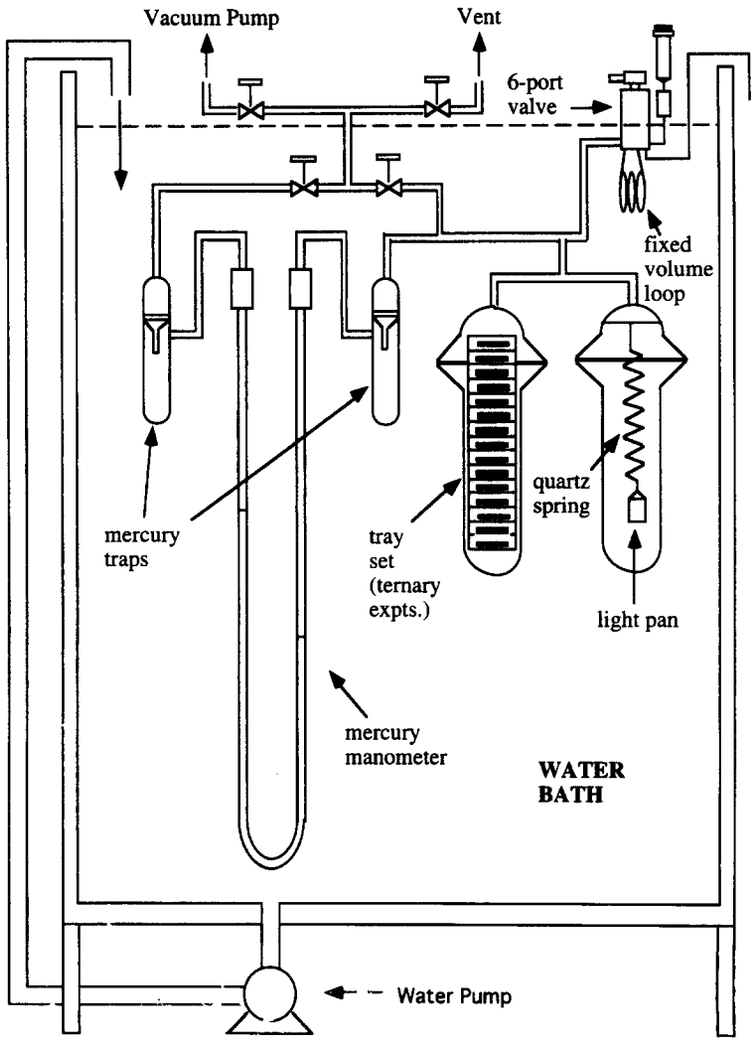

Figure 1 Experimental apparatus for VLE measurements for polymer + single solvent and polymer + binary solvent mixtures. (In single-solvent experiments, the tray set may be replaced with another polymer sample in a small pan suspended on a glass spring.)

Apparatus

Figure 1 shows a diagram of the VLE apparatus. It is based on the gravimetric–sorption method described by numerous authors, including Panayiotou and Vera[14] and Gupta and Prausnitz[15]. Polymer samples of known amount (20–30 mg) in aluminium pans are suspended on precalibrated quartz springs (Ruska Instruments Corp., Houston, TX, USA) inside evacuated glass chambers. The chambers are submerged in a fixed-temperature water bath and then evacuated to remove air, moisture and other volatile contaminants. Solvent vapour is introduced into the chambers through a

six-port switching valve (Rheodyne Inc., Cotati, CA, USA) with a filler port and a 200 μl sample loop. A 5 cm^3 syringe filled with liquid solvent is inserted into the filler port, and the solvent is injected into the sample loop. The valve handle is then turned, and the solvent vaporizes into the evacuated chambers. A mercury manometer measures the total vapour pressure in the chambers. Pressure and spring-length measurements are made as the system is allowed to equilibrate.

A cathetometer (Gaertner Scientific Corp., Chicago, IL, USA) is used to measure the extensions of the quartz springs. Calibration for each spring yields a linear relation between the mass of the spring load and the length of the spring. The springs have a maximum load of 200 mg and a sensitivity of approximately 1 mm mg^{-1}. The vernier scale on the cathetometer allows measurements to be made to the nearest hundredth of a millimetre. Hence, mass readings have a precision of 0.01 mg; for measurements reported here, solvent weight fractions in the liquid phase have an error of less than 1%. The cathetometer is also used to measure mercury levels in the manometer.

Experimental procedure for binary systems

The procedure for binary-system experiments is similar to that described by Gupta and Prausnitz[15]. Two different polymer samples may be used for each experimental run for faster data acquisition. Small aluminium pans are weighed on a microbalance. Polymer samples are placed in the pans; the chambers are then sealed and submerged in the water bath. The temperature of the bath is raised to 50°C, and the chambers are evacuated for several hours. The spring lengths are measured, and the polymer mass is precisely determined. Solvent is introduced into the chambers and allowed to equilibrate for 4–6 h. The system is considered to be at equilibrium when the spring length has not changed by more than ±0.05 mm over a 3 h period. At equilibrium, the spring extensions are measured to determine the amount of solvent that has condensed in the polymer sample. Pressure readings are made, and more solvent is added to the chambers until the total solvent weight fraction in the liquid phase is about 0.5 or until the system pressure is very close to the saturation vapour pressure of the solvent at 50°C.

Experimental procedure for ternary systems

In a ternary system, the mass of each solvent in either the liquid or vapour phase cannot be directly measured using the classical gravimetric–sorption method. That method gives only the total vapour pressure and the total solvent weight fraction in the liquid phase. Other measurements are required to determine mass fractions of the solvents in both phases.

For a ternary system, only one quartz spring and one type of polymer is used in each experimental run. The spring in the first chamber holds a 20–30 mg polymer sample as before. The spring in the second chamber is replaced with a set of 15 trays, each tray holding a polymer sample with a much larger amount (~200 mg) for a total of about 3 g. These larger polymer samples are placed in larger and wider aluminium pans to provide as much surface area to the vapour phase as possible. The samples in each large aluminium pan are weighed, placed in the trays, and the entire tray set is then sealed in the second chamber.

After introducing solvent into the chambers, the polymer + mixed solvent system is allowed to equilibrate for 3–5 days before more solvent is added. While nearly all of the absorption occurs in the first few hours, tiny changes in the weight of the liquid mixture in the small pan can still be measured after several days. This tiny change has little effect on the calculated solvent weight fraction in binary systems. However, small errors in the measured weight of the liquid mixture are magnified when calculating the weight fractions of each solvent in ternary systems, especially if the small and large polymer samples achieve equilibrium at different rates. The system is assumed to be at equilibrium when no more than a ±0.05 mm change in the spring length is observed over a 24 h period.

The 200 μl sample loop attached to the six-port switching value fixes the volume of the solvent introduced into the chambers each time. To determine accurately how much solvent is in the sample loop, the water level in the bath is lowered to expose the loop to room temperature air before the loop is filled with solvent. This ensures that the solvent will be a liquid at room temperature just before it is released into the chambers. The solvent is released, and the water level in the bath is restored. Knowing the room temperature, the liquid density of the solvent is established using correlated density data over a range of temperatures[16]. Multiplying the density by the volume of the sample loop yields the mass of solvent.

The volume occupied by the vapour phase is determined by introducing a volatile solvent into the apparatus at a fixed temperature with no polymer samples in the chambers. The temperature, pressure and moles of solvent molecules can be determined; these are used to calculate the volume of the system using the ideal-gas law.

Solvent weight fractions from ternary system data

In ternary-system experiments, the following set of mass-balance equations is used to determine the amount of each solvent in each phase:

$$m_{s1v} + m_{s1p} = m_{s1t} \tag{2}$$

$$m_{s2v} + m_{s2p} = m_{s2t} \tag{3}$$

$$\frac{PV}{RT} = \frac{m_{s1v}}{MW_1} + \frac{m_{s2v}}{MW_2} \tag{4}$$

$$\frac{m_{s1p} + m_{s2p}}{m_{pl} + m_{ph}} = \frac{m_{sl}}{m_{pl}} \tag{5}$$

m_{s1v} and m_{s1p} are the masses of solvent 1 in the vapour and liquid phases, respectively; m_{s2v} and m_{s2p} are the masses of solvent 2 in the vapour and liquid phases, respectively; and m_{s1t} and m_{s2t} are the total masses of solvent 1 and solvent 2 in the apparatus, respectively. P is the total pressure, V is the volume, R is the gas constant and T is the temperature. MW_1 and MW_2 are the molecular weights of solvents 1 and 2, respectively; m_{sl} and m_{pl} are the masses of the mixed solvent and the polymer in the small aluminium pan, respectively; and m_{ph} is the total mass of polymer in the set of trays. Equations (2) and (3) are mass-balance equations for solvents 1 and 2, respectively. Equation (4) assumes that the vapour phase is an ideal-gas mixture. Equation (5)

assumes that, at equilibrium, the ratio of mixed-solvent mass to polymer mass in the small aluminium pan is the same as that in all the large aluminium pans. The unknowns are m_{s1v}, m_{s1p}, m_{s2v} and m_{s2p}, while the remaining parameters are known or can be measured. Solving the equations simultaneously,

$$m_{s1v} = \frac{(PV/RT)MW_2 - (m_{s1t} + m_{s2t}) + m_{sl}(1 + m_{ph}/m_{pl})}{(MW_2/MW_1 - 1)} \quad (6)$$

$$m_{s2v} = \frac{(PV/RT)MW_1 - (m_{s1t} + m_{s2t}) + m_{sl}(1 + m_{ph}/m_{pl})}{(MW_1/MW_2 - 1)} \quad (7)$$

$$m_{s1p} = m_{s1t} - \frac{(PV/RT)MW_2 - (m_{s1t} + m_{s2t}) + m_{sl}(1 + m_{ph}/m_{pl})}{(MW_2/MW_1 - 1)} \quad (8)$$

$$m_{s2p} = m_{s2t} - \frac{(PV/RT)MW_1 - (m_{s1t} + m_{s2t}) + m_{sl}(1 + m_{ph}/m_{pl})}{(MW_1/MW_2 - 1)} \quad (9)$$

Equations (6)–(9) are then used to obtain the mass fraction of each solvent in each phase.

Accuracy of ternary system data

Assuming that the errors in molecular weights and total loading of each solvent are negligible, the error in the total mass of solvent 1 in the polymer phase can be evaluated by partial differentiation of equation (8):

$$\partial m_{s1p} = \frac{(PV/RT)MW_2(\partial P/P + \partial T/T + \partial V/V) + (1 + m_{ph}/m_{pl})\partial m_{sl}}{(MW_2/MW_1 - 1)} \quad (10)$$

The error in the weight fraction of solvent 1 in the polymer phase can be calculated as

$$w_1 = \frac{m_{s1p}}{m_{s1p} + m_{s2p} + m_{pl} + m_{ph}} \quad (11)$$

$$\partial w_1 = \frac{\partial m_{s1p}}{m_{s1p} + m_{s2p} + m_{pl} + m_{ph}} + \frac{(\partial m_{s1p} + \partial m_{s2p})m_{s1p}}{(m_{s1p} + m_{s2p} + m_{pl} + m_{ph})^2} \quad (12)$$

The second term on the right-hand side of equation (12) can be neglected since the denominator is much larger than the numerator. From equations (10) and (12),

$$\partial w_1 = \frac{(PV/RT)MW_2(\partial P/P + \partial T/T + \partial V/V) + (1 + m_{ph}/m_{pl})\partial m_{sl}}{(MW_2/MW_1 - 1)\frac{(m_{ph} + m_{pl})}{w_3}} \quad (13)$$

where w_3 is the weight fraction of the polymer. From equation (13), the accuracy of solvent weight-fraction calculations can be improved by increasing the total polymer mass, decreasing the volume of the vapour phase, and using solvents with very different molecular weights.

MOLECULAR-THERMODYNAMIC THEORY

A PHSC equation of state has been developed previously for pure fluids and fluid mixtures[17–20]. The PHSC model has been used to correlate VLE as well as liquid–liquid equilibrium data for homopolymer + solvent and copolymer + solvent systems[15]. In this model, molecules are chains of attracting hard spheres connected by covalent bonds. The total pressure, P, is the sum of several contributions:

$$P = P_{hs} + P_{ch} + P_{VdW} + P_{hb} \quad (14)$$

where P_{hs} is from hard-sphere repulsion, P_{ch} is from forming chains, P_{VdW} is from attractive van der Waals forces between non-bonded hard spheres and P_{hb} is from hydrogen-bonding interactions, if any. For binary and ternary polymer solutions, the general PHSC equation of state for heteronuclear chains with no hydrogen bonding is

$$\frac{P}{\rho k_B T} = 1 + \rho \sum_{i=1}^{m}\sum_{j=1}^{m} x_i x_j \left(\sum_{k=1}^{r_i}\sum_{l=1}^{r_j} b_{ij,kl} g_{ij,kl} \right) - \sum_{i=1}^{m} x_i \sum_{k=1}^{r_i - 1} (g_{ii,k,k+1} - 1) - \frac{\rho}{k_B T} \sum_{i=1}^{m}\sum_{j=1}^{m} x_i x_j \times \left(\sum_{k=1}^{r_i}\sum_{l=1}^{r_j} a_{ij,kl} \right) \quad (15)$$

where ρ is the number density, k_B is the Boltzmann constant, T is the absolute temperature, m is the number of components, x is the mole fraction, r is the number of spheres per molecule, b is a segment-size paramenter, g is the pair radial distribution function of hard spheres at contact and a is the attractive energy parameter. For a binary system, $m = 2$, and for a ternary system, $m = 3$. The subscripts ij, kl refer to the pair containing the kth segment of component i and the lth segment of component j. Parameters a and b are temperature-dependent as given by the Song–Mason method[21]. For pure solvents and homopolymers.

$$a = (2/3)\pi\sigma^3 \epsilon F_a(k_B T/\epsilon) \quad (16)$$

$$b = (2/3)\pi\sigma_3 F_b(k_B T/\epsilon) \quad (17)$$

where σ is the separation distance at the minimum potential energy and ϵ is the well depth of the pair potential. F_a and F_b are universal functions given by

$$F_a(k_B T/\epsilon) = 1.8681 \exp[-0.0619(k_B T/\epsilon)] + 0.6715 \exp[-1.7317(k_B T/\epsilon)^{3/2}] \quad (18)$$

$$F_b(k_B T/\epsilon) = 0.7303 \exp[-0.1649(k_B T/\epsilon)^{1/2}] + 0.2697 \exp[-2.3973(k_B T/\epsilon)^{3/2}] \quad (19)$$

For pairs of dissimilar segments A and B,

$$a_{AB} = (2/3)\pi\sigma_{AB}^3 \epsilon_{AB} F_a(k_B T/\epsilon_{AB}) \quad (20)$$

$$b_{AB} = (2/3)\pi\sigma_{AB}^3 F_b(k_B T/\epsilon_{AB}) \quad (21)$$

where

$$\sigma_{AB} = (1/2)(\sigma_A + \sigma_B)(1 - \lambda_{AB}) \quad (22)$$

$$\epsilon_{AB} = (\epsilon_A \epsilon_B)^{1/2}(1 - \kappa_{AB}) \quad (23)$$

λ_{AB} and κ_{AB} are adjustable binary intersegmental parameters. The pair correlation function is

$$g_{ij,kl} = \frac{1}{(1 - \eta)} + \frac{3}{2}\frac{\xi_{ij,kl}}{(1 - \eta)^2} + \frac{1}{2}\frac{\xi_{ij,kl}^2}{(1 - \eta)^3} \quad (24)$$

where the packing fraction η is

$$\eta = (\rho/4)\sum_{i=1}^{m} x_i \sum_{k=1}^{r_i} b_{i,k} \quad (25)$$

and

$$\xi_{ij,kl} = \frac{\rho}{4}\left(\frac{b_{i,k}b_{j,l}}{b_{ij,kl}}\right)^{1/3}\sum_{i=1}^{m} x_i \sum_{k=1}^{r_i} b_{i,k}^{2/3} \tag{26}$$

For systems with hydrogen-bonding interactions, P_{hb} can be calculated from the derivative of the Helmholtz energy of hydrogen bonding, A_{hb}:

$$P_{hb} = -\left(\frac{\partial A_{hb}}{\partial V}\right)_{\text{all}N_i,T} \tag{27}$$

The hydrogen-bonding Helmholtz energy proposed by Veytsman[22–24] and modified by Gupta and Johnston[25] is

$$\frac{A_{hb}}{RT} = \sum_k \sum_l N_{kl}\left(1 + \frac{F_{kl}^0}{RT} + \ln\frac{N_{kl}\sum_t r_t N_t}{N_{k0}N_{0l}} - \ln(g_{ij}\eta)\right) + \sum_k N_d^k \ln\frac{N_{k0}}{N_d^k} + \sum_l N_a^l \ln\frac{N_{0l}}{N_a^l} \tag{28}$$

Here, N_{kl} is the number of kl hydrogen bonds; g_{ij} is the pair radial distribution function where i is the segment that contains donor group k and j is the segment that contains acceptor group l; and N_t is the number of t molecules. F_{kl}^0 is the standard Helmholtz energy of hydrogen bonding given by

$$F_{kl}^0 = E_{kl}^0 - TS_{kl}^0 \tag{29}$$

where E_{kl}^0 and S_{kl}^0 are the standard energy and entropy of hydrogen bonding, respectively. N_{k0} and N_{0l} are the number of unbonded donor and acceptor sites, respectively, given by

$$N_{k0} = N_d^k - \sum_{l=1}^{m} N_{kl} \tag{30}$$

$$N_{0l} = N_a^l - \sum_{k=1}^{n} N_{kl} \tag{31}$$

where N_d^k is the total number of k donor sites, N_a^l is the total number of l acceptor sites, m is the number of kinds of acceptor sites and n is the number of kinds of donor sites. The number of hydrogen bonds N_{kl} between donor group k and acceptor group l is determined by minimizing the Gibbs energy with respect to all kl bonds:

$$\frac{N_{kl}\sum_t r_t N_t}{N_{k0}N_{0l}} = \eta g_{ij}\ \exp\left(\frac{-G_{kl}^0}{RT}\right) \tag{32}$$

where

$$G_{kl}^0 = E_{kl}^0 - TS_{kl}^0 + PV_{kl}^0 \approx F_{kl}^0 \tag{33}$$

Here, V_{kl}^0 is the hydrogen-bonding volume parameter. At low or moderate pressures, the PV_{kl}^0 term is negligible.

In summary, each pure solvent and monomer is characterized by three molecular constants: r, σ and ϵ. Constants for 77 solvents and 22 homopolymers have been obtained previously from pure-component thermodynamic properties such as vapour pressures and liquid and vapour densities[20].

For non-hydrogen-bonding systems, each unlike pair of segments requires one or two binary parameters (κ and λ) to be determined from binary data. In many cases, only one parameter (λ) is used to fit the VLE data. For a hydrogen-bonding system at constant temperature, each type of hydrogen-bonding interaction requires one parameter F^0. The effect of temperature on F^0 is given by E^0 and S^0. All data reported here are at 50°C; κ, λ and F^0 are determined from experimental binary mixture data.

Table 2 Vapour–liquid equilibrium data for binary polymer + solvent systems at 50°C (w_1 = solvent weight fraction in liquid phase, P = pressure, kPa)

w_1	P
Acetone + PS[a]	
0.071	45.75
0.079	47.95
0.103	55.14
0.155	66.34
0.253	76.39
0.352	79.90
0.429	81.13
Acetone + PMMA	
0.074	35.32
0.099	46.57
0.135	56.21
0.195	64.99
0.267	72.02
0.356	77.71
Acetone + P(S-*co*-MMA)	
0.074	51.98
0.126	64.30
0.231	76.06
0.445	81.67
Methyl acetate + PS	
0.062	29.17
0.103	43.06
0.159	56.38
0.244	68.25
0.351	76.05
Methyl acetate + PMMA	
0.094	29.17
0.133	43.06
0.204	56.38
0.311	68.25
0.442	76.05
Methyl acetate + P(S-*co*-MMA)	
0.081	43.10
0.121	52.81
0.174	61.39
0.246	68.83
0.321	74.73
Chloroform + PS[b]	
0.203	28.47
0.295	38.94
0.361	45.71
0.432	52.41
0.433	52.06
0.546	60.37
0.644	65.19
0.707	67.07
Chloroform + PMMA	
0.167	14.36
0.288	27.96
0.431	40.43
0.562	51.86
0.678	60.79
Chloroform + P(S-*co*-MMA)	
0.116	14.36
0.251	27.96
0.374	40.43
0.508	51.86
0.624	60.79

[a] Data from Bawn and Wajid[26] M_w = 15 700
[b] Data from Bawn and Wajid[26] M_w = 290 000

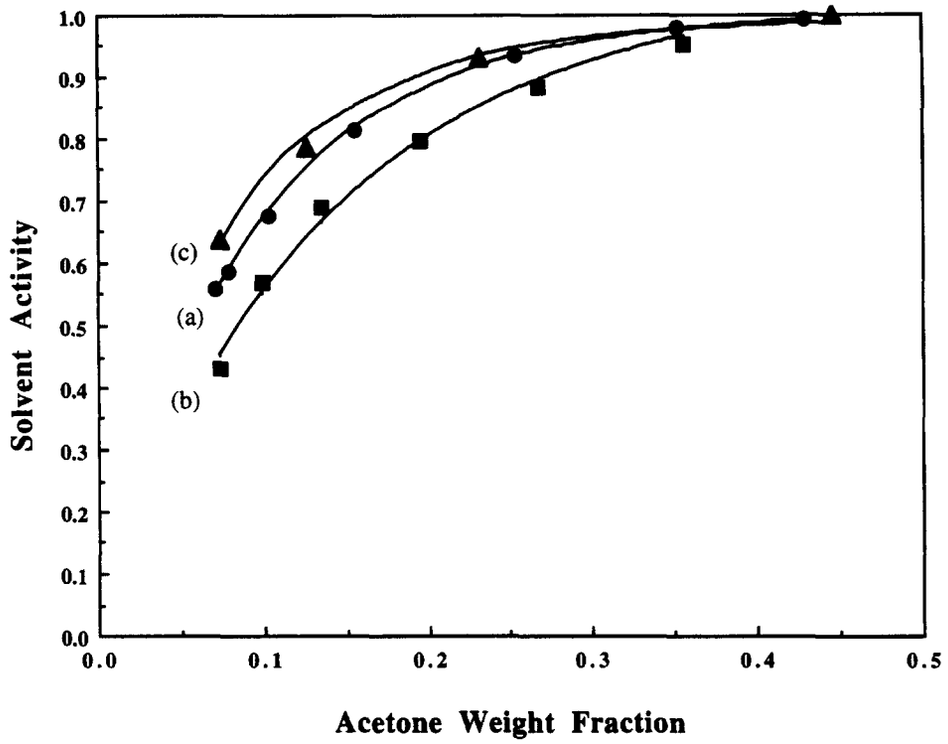

Figure 2 VLEs for (a) PS, (b) PMMA and (c) P(S-*co*-MMA) in acetone at 50°C; data for (a) from Bawn and Wajid[26]. Symbols, experimental data. Lines, calculation using the PHSC equation-of-state parameters: PS + acetone, $\kappa = 0.06540$, $\lambda = -0.07015$; PMMA + acetone, $\kappa = 0.01690$, $\lambda = -0.04351$; PS + PMMA, $\kappa = -0.06940$, $\lambda = 0.06633$

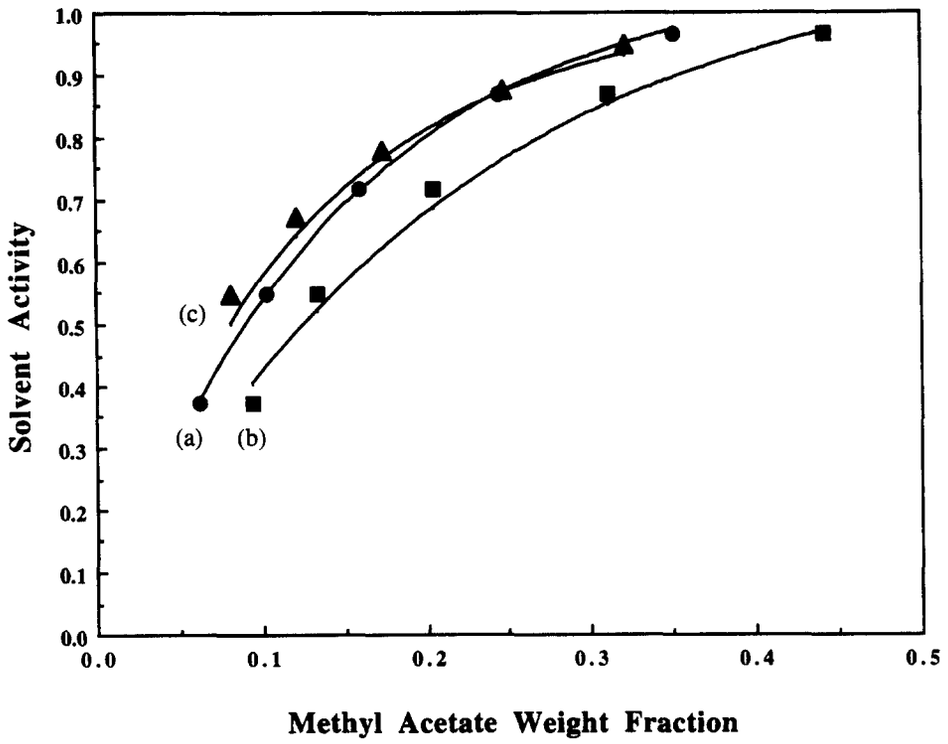

Figure 3 VLEs for (a) PS, (b) PMMA, and (c) P(S-*co*-MMA) in methyl acetate at 50°C. Symbols, experimental data. Lines, calculation using the PHSC equation-of-state parameters: PS + methyl acetate, $\kappa = 0.03873$, $\lambda = -0.04231$; PMMA + methyl acetate, $\kappa = 0$, $\lambda = -0.03358$; PS + PMMA, $\kappa = -0.06940$, $\lambda = 0.06633$

RESULTS AND DISCUSSION

Binary systems

Table 2 lists the binary data acquired in this work and correlated using the PHSC equation of state. High molecular-weight polymers are used here to minimize the effect of polymer molecular weight on VLE behaviour, especially for systems with strong polymer–solvent interactions[27]. The polymers used here have glass-transition temperatures of 100°C or more; at 50°C, they change from powder form into the liquid state only

when enough solvent is present in the system. We therefore confine our attention to those data where the solvent weight fraction is at least 5%.

Figure 2 shows the solvent activity P/P_{sat} (P_{sat} = saturation pressure of the solvent at the given temperature) as a function of solvent weight fraction for P(S-*co*-MMA) and its parent homopolymers in acetone at 50°C. At given activity, acetone absorption is largest for PMMA and smallest for P(S-*co*-MMA). Solvent solubility is high for PMMA due to favourable polar interactions between acetone and the ester group on the methyl methacrylate (MMA) segments. Such interactions are absent for styrene (ST) and acetone; therefore, polar solvents are less soluble in PS. Intuitively, one might expect that the solubility of a solvent in the copolymer would lie between those in its parent homopolymers, but that is not the case here. Binary parameters κ and λ for all non-identical segment pairs were regressed from binary experimental data. The curves in *Figure 2* show that the data are well represented by the PHSC equation of state. Binary parameters regressed for the ST–MMA pair from copolymer–acetone data are used to predict VLEs for solutions of the copolymer in methyl acetate and chloroform.

Figure 3 shows VLEs for the polymers in methyl acetate at 50°C. For a fixed solvent activity, methyl acetate is more soluble in the polymers than acetone because methyl acetate has a slightly lower vapour pressure than acetone. The ester carbonyl group in methyl acetate is more polar than the carbonyl group in acetone, giving stronger attraction between an MMA segment and methyl acetate. Solvent solubility in P(S-*co*-MMA) is lower than that for either parent homopolymer. Binary parameters κ and λ were regressed for both methyl acetate segment pairs using solubility data for methyl acetate in the homopolymers. Using the binary parameters regressed for the ST–MMA pair from copolymer + acetone data, good agreement was found between the predicted VLE curve and the experimental data for P(S-*co*-MMA) + methyl acetate.

A molecular explanation has been suggested previously to rationalize how a solvent can be more soluble in a copolymer than in either of its parent homopolymers[13]. The polar and non-polar sections of a solvent molecule can each interact favourably with the corresponding polar and non-polar segments of the copolymer chain, increasing solvent absorption. In the P(S-*co*-MMA) + methyl acetate system, the ester group on methyl acetate has energetically favourable interactions with the MMA segments. The methyl groups on methyl acetate, however, do not have strong attraction with the PS segments. Considering only these interactions, solvent absorption by the copolymer should be at least between solvent absorption by PS and PMMA, and perhaps larger.

However, there may be another important molecular consideration. The copolymer chain is in a highly coiled conformation at low solvent concentrations. MMA segments interact strongly with each other along the copolymer chain. When small amounts of solvent are added, these strong interactions maintain the coiled conformation of the copolymer. Even with favourable interactions between acetone or methyl acetate with MMA, there is only a small gain in the entropy of the copolymer chain when solvent is added at low concentrations. Further, in the copolymer, the aromatic rings on PS are subject to repulsive forces from the polar MMA segments, resulting in a loss in the mobility of the ST rings. Infrared dichroism experiments on uniaxially stretched styrene-*co*-methyl methacrylate

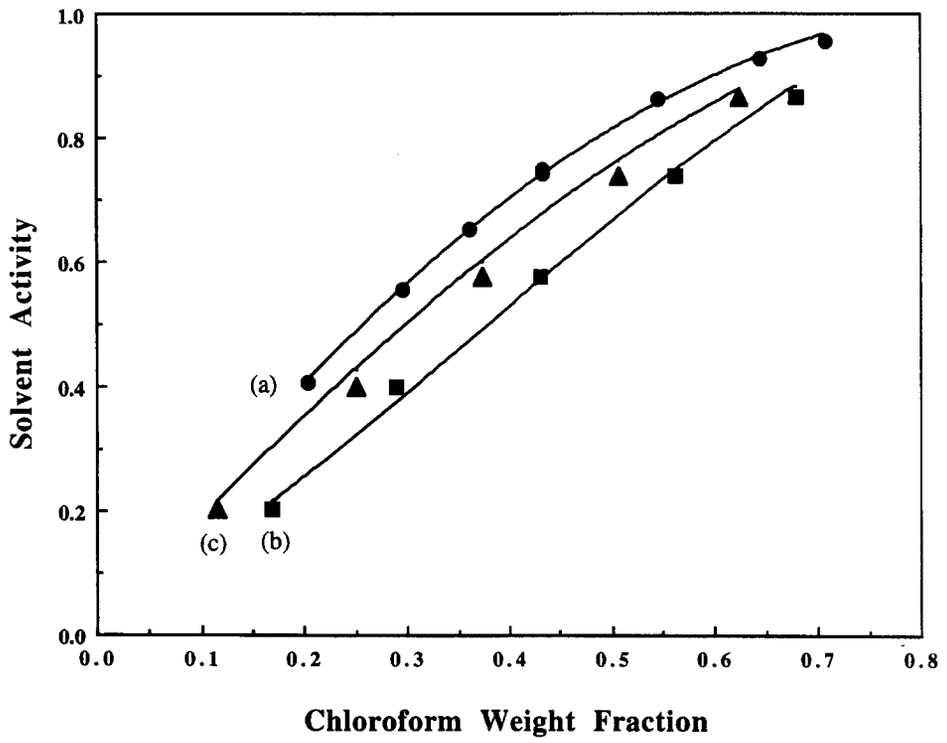

Figure 4 VLEs for (a) PS, (b) PMMA, and (c) P(S-*co*-MMA) in chloroform at 50°C; data for (a) from Bawn and Wajid[26]. Symbols, experimental data. Lines, calculation using the PHSC equation-of-state parameters: PS + chloroform, $\kappa = 0$, $\lambda = -0.02418$; PMMA + chloroform, $F^0/R = 27.89$ K, $\kappa = 0$, $\lambda = -0.04098$; PS + PMMA, $\kappa = -0.06940$, $\lambda = 0.06633$

Table 3 Vapour–liquid equilibrium data for the PS + chloroform + tetrachloride system at 50°C

Experimental data				Correlated results[a]	
w_1	w_2	y_1	P	y_1	P
0.154	0.176	0.436	40.13	0.438	38.06
0.187	0.202	0.451	44.22	0.418	43.59
0.206	0.238	0.429	47.44	0.428	47.82
0.234	0.257	0.443	50.00	0.413	51.58

[a] PHSC equation-of-state parameters: PS + chloroform, $\kappa = 0$, $\lambda = -0.02418$; PS + carbon tetrachloride, $\kappa = 0$, $\lambda = -0.02576$; chloroform + carbon tetrachloride, $\kappa = 0$, $\lambda = 0.04250$
w_1, liquid weight fraction of chloroform
w_2, liquid weight fraction of carbon tetrachloride
y_1, vapor mole fraction of chloroform
P, total vapour pressure (kPa)

random copolymers show that as the MMA content of the copolymer increases, the orientation of ST segments also increases[28]. This orientation of the PS segments in the random copolymer arises from the intramolecular repulsion from the polar MMA segments. Birefringence measurements also show that for an MMA content of more than 50% in the copolymer, a change in the PS ring orientations occurs due to significant steric hindrance to the motion of the aromatic ring[28]. Addition of acetone and methyl acetate, which are structurally similar to the polar methacrylate group of MMA, further enhances the polar environment around the PS rings. These entropically unfavourable effects on the overall copolymer chain and the rings may explain why acetone and methyl acetate are less soluble in P(S-*co*-MMA) than in homopolymer PS or PMMA at low solvent concentrations.

At higher solvent concentrations, the equation of state predicts that acetone and methyl acetate may become slightly more soluble in P(S-*co*-MMA) than in PS. As more solvent is absorbed, the copolymer chain acquires a more relaxed conformation, and the entropic effects from MMA–MMA segment interactions may decline. Our experimental data could not confirm this decline because vapour pressures are very near saturation even at low solvent concentrations. At higher solvent concentrations, solvent weight fraction measurements become very sensitive to small fluctuations in temperature and pressure.

Figure 4 shows VLEs for the polymers in chloroform at 50°C. These results are similar to those for poly(styrene-*co*-50% butyl methacrylate) and its parent homopolymers in chloroform[15]. Chloroform is a good solvent for both PS and PMMA. The VLE curve for P(S-*co*-MMA) is between those for PS and PMMA but much closer to PMMA due to strong polar interactions between chloroform and the MMA monomers. There is evidence that chloroform can form hydrogen bonds with strong bases such as pyridine and triethylamine[29]. It may be possible for chloroform to form weak hydrogen bonds with MMA. It is useful to interpret the VLE data using the Veytsman model. One binary parameter, λ, was sufficient to correlate PS + chloroform VLE data. For the PMMA + chloroform and P(S-*co*-MMA) + chloroform systems, parameters F^0 and λ were regressed. The value obtained for F^0 is of the same order as that reported for typical hydrogen-bonding systems at 50°C[29].

Ternary system

VLE data for the PS + chloroform + carbon tetrachloride system were obtained at 50°C. A 200 μl volume of chloroform was first introduced into the apparatus, and then 200 μl of carbon tetrachloride was added. More chloroform and carbon tetrachloride were added in this alternating fashion until the total solvent weight fraction reached 0.5. This ensures that there would be comparable amounts of both solvents in the mixture. Because the estimated errors in low solvent weight fractions were large, we consider only data with total solvent weight fractions in the liquid phase larger than 25%.

Table 3 gives the experimental liquid mass fractions, vapour composition and total pressures obtained for the PS + chloroform + carbon tetrachloride system at 50°C. Vapour composition and pressures calculated from the experimental liquid-phase composition using the PHSC equation of state are compared with experimental results. Optimizing parameter λ of the chloroform–carbon tetrachloride pair yields a root-mean-square deviation of 5% between calculated and observed partial pressures.

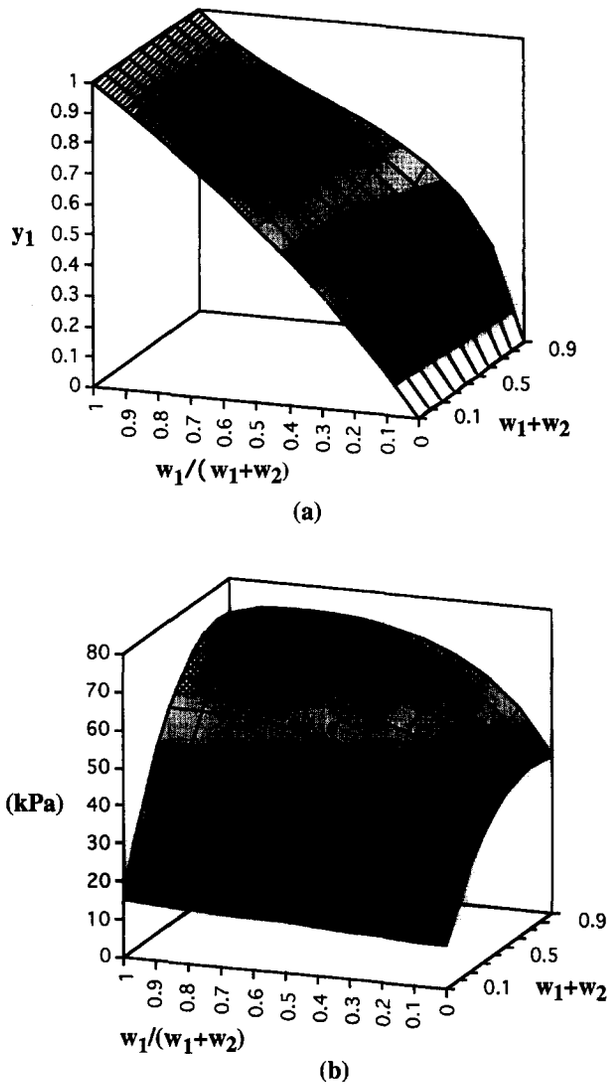

Figure 5 (a) Vapour composition and (b) total vapour pressure for the system PS + chloroform + carbon tetrachloride at 50°C. w_1 and w_2, weight fractions of chloroform and carbon tetrachloride in the polymer phase, respectively; y_1, mole fraction of chloroform in the vapour phase. Calculations based on PHSC equation-of-state parameters: PS + chloroform, $\kappa = 0$, $\lambda = -0.02418$; PS + carbon tetrachloride, $\kappa = 0$, $\lambda = -0.02576$; chloroform + carbon tetrachloride, $\kappa = 0$, $\lambda = 0.04250$

Figure 5 shows contour plots of the predicted total vapour pressures and vapour compositions of the PS + chloroform + carbon tetrachloride system over the entire range of total solvent weight fractions and compositions in the liquid phase at 50°C. Shading is provided to aid visualization. VLE data for PS + chloroform at 50°C[26], PS + carbon tetrachloride at 20°C[30], and PS + chloroform + carbon tetrachloride at 50°C were used to regress the binary parameters for the PHSC equation of state. Three of the four sides of the contour plots correspond to the predicted VLEs of PS + chloroform, PS + carbon tetrachloride and chloroform + carbon tetrachloride mixtures. For a fixed total solvent weight fraction, the total vapour pressure rises as the amount of chloroform in the liquid phase increases because chloroform is more volatile than carbon tetrachloride. Although chloroform has a higher vapour pressure, it has a permanent dipole moment (1.05 debye)[31] unlike carbon tetrachloride and interacts more strongly with polarizable aromatic rings. Thus, the plots show that chloroform becomes preferentially absorbed with increasing amounts of PS in the liquid mixture.

CONCLUSIONS

New binary VLE data have been obtained for P(S-*co*-MMA) and PMMA in acetone, methyl acetate and chloroform, as well as for PS in methyl acetate. Normal behaviour was observed for chloroform in P(S-*co*-MMA), but acetone and methyl acetate show diminished solubility in the copolymer compared to those in PS and PMMA. The combined effects of polar MMA segment and polar solvent interactions on the motion of the aromatic rings and conformation of the copolymer chain cause a loss in the entropy of the copolymer, resulting in a decrease in acetone and methyl acetate absorption. Ternary VLE data were also obtained for the PS + chloroform + carbon tetrachloride system. The PHSC equation of state can represent VLEs of both binary and ternary polymer + solvent mixtures. It can correlate both normal and reduced absorption of solvents in copolymers.

ACKNOWLEDGEMENTS

This work was supported by the Director, Office of Energy Research, Office of Basic Energy Science, Chemical Science Division of the US Department of Energy under contract No. DE-AC03-76SF0098. The authors are grateful for additional financial support from the donors of the Petroleum Research Fund (administered by the American Chemical Society), E. I. du Pont de Nemours (Philadelphia, PA), Koninklijke Shell (Amsterdam, The Netherlands) and the National Science Foundation. Special thanks are due to Ram Gupta for development of the experimental procedures and for help with equipment design, and to Stephen Lambert and Burkhard Schäfer for providing source codes for the correlation of experimental data.

REFERENCES

1. Baker, R. W., Yoshioka, N., Mohr, J. M. and Kahn, A. J., *J. Membr. Sci.*, 1987, **31**, 259.
2. Matsumoto, K., Ishii, K., Koruda, T., Inoue, K. and Iwama, A., *Polym. J.*, 1991, **23**, 491.
3. Ballantine, D. S., Jr and Wohltjen, H., *Anal. Chem.*, 1989, **61**, 704.
4. Grate, J. W., Klusty, M., McGill, R. A., Abraham, M. H., Whiting, G. and Andonian-Haftvan, J., *Anal. Chem.*, 1992, **64**, 610.
5. High, M. S. and Danner, R. P., *Fluid Phase Equilibria*, 1990, **55**, 1.
6. Kubota, H., Yoshino, N. and Ogiwara, Y., *J. Appl. Polym. Sci.*, 1990, **39**, 1231.
7. Maeda, Y., Tsuyumoto, M., Karakane, H. and Tsugaya, H., *Polym. J.*, 1991, **23**, 501.
8. Bonner, D. C. and Prausnitz, J. M., *J. Polym. Sci.*, 1974, **21**, 51.
9. Corneliussen, R., Rice, S. A. and Yamakawa, H., *J. Chem. Phys.*, 1963, **38**, 1768.
10. Wolfarth, C., *Vapour–Liquid Equilibrium Data of Binary Polymer Solutions, Vapour–Pressures, Henry-constants and Segment-molar Excess Gibbs Free Energies*. Elsevier, Amsterdam, 1994.
11. ten Brinke, G., Karasz, F. E. and MacKnight, W. J., *Macromolecules*, 1983, **16**, 1827.
12. Paul, D. R. and Barlow, J. W., *Polymer*, 1984, **25**, 487.
13. Gupta, R. B. and Prausnitz, J. M., *Fluid Phase Equilibria*, 1996, **117**, 77.
14. Panayiotou, C. G. and Vera, J. H., *Polym. J.*, 1984, **16**, 89.
15. Gupta, R. B. and Prausnitz, J. M., *J. Chem. Eng. Data*, 1995, **40**, 784.
16. Daubert, T. E. and Danner, R. P., *Physical and Thermodynamic Properties of Pure Chemicals: Data Compilation*. Hemisphere, New York, 1990.
17. Song, Y., Lambert, S. M. and Prausnitz, J. M., *Macromolecules*, 1994, **27**, 441.
18. Song, Y., Lambert, S. M. and Prausnitz, J. M., *Ind. Eng. Chem. Res.*, 1994, **33**, 1047.
19. Song, Y., Lambert, S. M. and Prausnitz, J. M., *Chem. Eng. Sci.*, 1994, **49**, 2765.
20. Song, Y., Hino, T., Lambert, S. M. and Prausnitz, J. M., *Fluid Phase Equilibria*, 1996, **117**, 69.
21. Song, Y. and Mason, E. A., *J. Chem. Phys.*, 1989, **91**, 7840.
22. Veytsman, B. A., *J. Phys. Chem.*, 1990, **94**, 8499.
23. Panayiotou, C. G. and Sanchez, I. C., *J. Phys. Chem.*, 1991, **95**, 10090.
24. Gupta, R. B., Panayiotou, C. G., Sanchez, I. C. and Johnston, K. P., *AIChE J.*, 1992, **38**, 1243.
25. Gupta, R. B. and Johnston, K. P., *Fluid Phase Equilibria*, 1994, **99**, 135.
26. Bawn, C. E. and Wajid, M. A., *Trans. Faraday Soc.*, 1956, **52**, 1658.
27. Wang, K., Hu, Y. and Wu, D. T., *J. Chem. Eng. Data*, 1994, **39**, 916.
28. Oultache, A. K., Jasse, B. and Monnerie, L., *J. Polym. Sci. B: Polym. Phys.*, 1994, **32**, 2539.
29. Pimentel, G. C. and McClellan, A. L., *The Hydrogen Bond*. Freeman, San Francisco, 1960.
30. Baughan, E. C., *Trans. Faraday Soc.*, 1948, **44**, 495.
31. Prausnitz, J. M., Lichtenthaler, R. N. and de Azevedo, E. G., *Molecular Thermodynamics of Fluid-Phase Equilibria*. Prentice Hall, New Jersey, 1986.